Biomechanical Analysis of Fibular Graft Techniques for Nontraumatic Osteonecrosis of Femoral Head: A Finite Element Analysis

Jian Xu
Shanghai Jiao Tong University Affiliated Sixth People's Hospital
Shi Zhan
Shanghai Jiao Tong University Affiliated Sixth People's Hospital
Ming Ling
Fudan University Affiliated Heading Hospital
Dajun Jiang
Shanghai Jiao Tong University Affiliated Sixth People's Hospital
Hai Hu (xmhuhai@hotmail.com)
Shanghai Jiao Tong University Affiliated Sixth People's Hospital https://orcid.org/0000-0002-4759-9730
Jiagen Sheng
Shanghai Jiao Tong University Affiliated Sixth People's Hospital
Changqing Zhang
Shanghai Jiao Tong University Affiliated Sixth People's Hospital

Research article

Keywords: Osteonecrosis of the femoral head; free vascularized fibula graft; surgical techniques; finite element analysis

Posted Date: July 2nd, 2020

DOI: https://doi.org/10.21203/rs.3.rs-39636/v1

Version of Record: A version of this preprint was published on August 17th, 2020. See the published version at https://doi.org/10.1186/s13018-020-01867-4.

Abstract

Background: Free vascularized fibula graft (FVFG) technique has achieved the most consistent successful therapeutic effect on young patients diagnosed as nontraumatic osteonecrosis of femoral head (NONFH), of which the Core Track Technique (CTT) has been the most commonly used. As an alternative to CTT, the modified Light Bulb Technique (LBT) was reported to have a higher success rate. However, its biomechanical characters have been poorly understood. This study aimed to investigate the biomechanical properties of modified LBT in treating NONFH by comparing with CTT.

Methods: Two types (C1 and C2) of NONFH finite element models were established from a healthy subject according to the Japanese Investigation Committee (JIC) classification, and CTT and LBT procedures were simulated in each type of the models. The average Von Mises stresses and stiffness of the proximal femur were calculated by applying 250% body weight loading on femoral head to simulate walking condition. In addition, two patient-specific models were built and simulated under the same boundary condition for the further validation of LBT.

Results: In the healthy subject-derived models, both LBT and CTT resulted in reduced stresses in the weight-bearing area, central femoral head, femoral neck, and trochanteric and subtrochanteric regions, and increased structural stiffness after surgery. In the weight-bearing area, CTT reduced more stresses than LBT (36.19% *vs* 31.45%) for Type C1, while less reduction (23.63% *vs* 26.76%) for Type C2. In patient-specific models, stiffness and stresses of before and after surgery were also increased and reduced respectively, which is consistent with healthy subject-derived models.

Conclusion: LBT and CTT have different biomechanical performance on different JIC type of NONFH. In terms of preventing the collapse of femoral head, LBT may be more effective for JIC Type C2, which could alternatively be chosen, while for JIC Type C1, CTT is still a better choice. Both techniques can improve biomechanical properties of NONFH with patients' proximal femur stress reduced and structural stiffness enhanced.

1. Background

Nontraumatic osteonecrosis of femoral head (NONFH) is a common disabling disease mainly affecting young individuals, which is caused by insufficient blood supply and leads to femoral head collapse and premature osteoarthritis[1–3]. Various preservation procedures have been tried to prevent the femoral head from collapse. If so, hip replacement becomes unavoidable, which is reluctant for young patients due to revision surgery and financial burden[4,5]. Among the preservation procedures, free vascularized fibula graft (FVFG) has achieved the most consistent successful therapeutic effect on the treatment of early NONFH, which includes the removal of necrotic lesion under weight-bearing area, buttressing articular surface by grafted fibula and revascularization of femoral head[2,6–10].

Current procedures of FVFG mainly include Core Tack technique (CTT)[11] and modified Light Bulb technique (LBT)[10], with success rates of 60%-90% and 94.6%-96%, respectively[2,10–13]. CTT is the most commonly used technique for treating NONFH, which is fulfilled by drilling a core tunnel from the lateral aspect of the greater trochanter, removing necrotic bone tissue and implanting bone. However, this technique reams more healthy bone, harvests longer fibula graft, demands a longer fibular pedicle and a longer operation duration. As an alternative to CTT, LBT is applied, which initially described by Rosenwasser[14] and subsequently modified by Zhang and his colleagues as one of the FVFG techniques[10]. To implement the modified LBT, a window is opened in the anterolateral cortex of the femoral neck. Anatomically, lateral femoral circumflex vessel is constantly located in this anterior approach, which favorably allows less donor and shorter fibular pedicle[13]. In a LBT long-term follow-up study, Gao et al[10] reported that 91% (526/578) of the femoral heads remained in shape or even improved postoperatively in radiographic evaluation. Although LBT contributed to a relative higher success rate compared with CTT, Aldridge et al[15] argued that LBT could rise the stress by opening an anterior window. To the best of our knowledge, no quantitative study exists regarding the biomechanical benefit of LBT, whose biomechanical characters have been poorly understood.

In this study, we aimed to investigate biomechanical effects of LBT in the treatment of NONFH in comparison with CTT. The hypothesis was that the higher success clinical rate of LBT was partly attributed to its better biomechanical characters when applied for a certain type of NONFH.

2. Method

2.1 Establish the initial 3D model

A healthy male volunteer, aging 35, 178 cm in height, 75 kg in weight, was recruited, who has no history of hip trauma, no hormone taking history and no long-term alcohol-drinking history. The experiment is under the volunteer's consent and approved by local ethics committee. His hip health was confirmed by anteroposterior pelvis X-ray, full length X-ray image of bilateral lower extremities, and thin-slice CT scan (SOMATOM Definition AS1; Siemens). The left lower limb was scanned from pelvis to feet to obtain CT data of a thin layer with a resolution of 512 × 512 in pixels and a layer thickness of 0.625 mm. In Mimics 19.0 (Materialise Ltd., Leuven, Belgium), segmentation techniques were used to reconstruct 3D models of hip, femur, and fibula.

2.2 Classify necrosis lesions of femoral head

Necrosis lesions are classified into four visualized types (Type A, B, C1, and C2), based on their location relative to the weight-bearing area in according with Japanese Investigation Committee (JIC) classification[16]. In the JIC classification, Type C1 and C2 are recommended to undergo joint-preserving therapies. Thus, they were employed in this study, and established based on the 3D finite element model of the normal upper femur, respectively (Fig. 1a, b, c). Each necrotic domain volume was 30% of femoral head, as a prerequisite for the intervention of femoral head collapse[17].

2.3 Simulation of CTT and LBT

In the two types of necrotic groups, total four post-operation models were simulated under CTT and LBT surgical technique, respectively (Fig. 1d, e). Models were simulated using the Boolean operations as virtual surgical procedures in 3-Matic 11.0 (Materialise Ltd., Leuven, Belgium). CTT drilled a core along the axis of femoral neck starting from the lateral cortex as the approximately 2 cm distal to the vastus ridge, and into the necrosis lesion in the femoral head[11,18]. LBT opened a window at the anterior aspect of the femoral neck which should match the grafted fibula, with the size 3 × 1.5 × 1.5 cm. A bone tunnel was made along the axis of the femoral neck from window deep into the necrosis lesion in the femoral head[10,13]. The debridement region removed with the burr was the 1/2 radius of the necrotic domain[19]. The grafted fibular dimensions (length as in the Table 1 and fitting radius as 6.8 mm) were obtained from the volunteer's CT images. The direction of fibular axis was defined by the starting point which was located in different procedures starting place, and the ending point which was located in central position of the weigh-bearing portion in necrotic lesions on anteroposterior and medial-lateral views. The distance between the cortical bone and the apical tip of the fibula was 5 mm[20]. The impaction cancellous bone was filled by remaining voids.

Table 1
Length of grafted fibular and model elements

	JIC C1 Group			JIC C2 Group		
	Preoperation	CTT	LBT	Preoperation	CTT	LBT
Length*	-	9.43	6.53	-	9.53	6.27
Element	386995	461922	417666	384123	452905	435146
Node	81528	98634	89455	80980	97152	93317
*: Length of grafted fibular (cm).						

2.4 Finite element analysis

All finite element analysis (FEA) models created a 1-mm mesh size in Abaqus/Standard 6.14 (SIMULIA Co., Providence, RI, USA). The number of elements and nodes of each FEA model is shown in Table 1. There was a linear correlation between bone density and Hounsfield Unit. Bone density is related to material properties. Hence, the material properties of each femoral model were based on the level of Hounsfield Unit from CT scan data[21]. The mathematical formulas are as follows: (see Formulas 1-3 in the Supplementary Files)

The fibula, necrotic bone and cancellous bone were assigned to different material properties which obtained from other studies[19,22,23]. In these models, each part was assumed to be linear elastic, homogeneous and isotropic. Their moduli of elasticity were 15100 Mpa, 124.6 Mpa, 445 Mpa; and their

Poisson's ratio were 0.3, 0.152, and 0.22, respectively. There was no gap around the interfaces between the grafted bone and femur in all postoperative models.

To simulate the real situation of the hip joint, each FEA femoral model had been fixed in standing position. The same reference point upon the weight-bearing area was set, and the elliptical area at the junction of the femoral head and the acetabulum was set to couple the entire weight-bearing area, in which the arc of the area towards the center of the femoral head was 85 degree in medial-lateral views and anteroposterior views. A force of 250% body weight was loaded on the reference point along the mechanical axis of the femur to simulate hip joint reaction force during the normal walking[24], and the distal femur was fully restrained to movement (Fig. 2a).

In this study, for each model, the average von Mises stress in the mechanical conditions of the femur was calculated from all the elements in four different regions: a) weight-bearing area, b) central femoral head, c) femoral neck and d) trochanteric and subtrochanteric region[25] (Fig. 2b). The structural stiffness was obtained from the ratio of the force to the displacement of the reference point, reflecting the ability of the proximal femur to resist deformation. The maximum principal strain at each element of the proximal femur was calculated to observe the risk of fracture in each region in comparison with ultimate compressive strain (0.0104) and ultimate tensile strain (0.0073) from references[25,26].

2.5 Validation of patient-specific models

To verify the finite element models, two patients diagnosed bilateral NONFH were enrolled from our hospital (Table 2), classified as Type C1 and C2, respectively, according to JIC classification (both in stage 2, Fig. 3a, e), using the same FEA method to compare the average stress of different regions before and after surgery with LBT. Preoperative and 4 weeks postoperative CT scan data were obtained for analysis.

Table 2
Patient parameter

Parameter	Paitient-1	Paitient-2
Sex	Female	Female
Age	38	21
Height (cm)	155	160
Weight(Kg)	55	50
BMI	22.8	19.5
Bilateral	yes	yes
Surgical hip	Right	Left
JIC Classification	Type C1	Type C2
Length of grafted fibular (cm)	6.67	7.13
FEA	Pre/post operation	
Element	250814/257049	235848/251905
Node	52100/53402	49077/52590

3. Results

As shown in Fig. 4a, in the simulation of maximal walking impact, the relatively high stresses appeared mainly from the weight-bearing area to calcar in the healthy model, forming the normal stress transfer path of the proximal femur. However, the stress transfer path was blocked off in necrotic models. After implementing CTT/LBT, the implanted fibular graft bore partially the high stresses and contributed to the reconstruction of the stress transfer path.

In all postoperative simulation models, the average von Mises stress was alleviated in all four regions (Fig. 5 & Table 3), and the most reduced was in weight-bearing area (23.63%-36.19%). Among those, CTT had greater reduction than LBT in JIC C1 group (36.19% *vs* 31.45%), whereas LBT had greater reduction than CTT in JIC C2 group (26.76% *vs* 23.63%). In other regions, CTT led a greater reduction of stresses in both JIC C1 and JIC C2 groups in comparison with LBT (range of reduction, 12.86%-23.48% *vs* 2.51%-20.43%). The stiffness increased in both CTT and LBT (2.26%-9.40%), and the increase for CTT was greater than that for LBT in both types of necrosis (Table 3). There were no yielding units postoperatively appeared in proximal femur.

Table 3
The average Von Mises stress and stiffness in each region and reduced percentage in CTT and LBT

	Stress (Mpa)				Stiffness
	WB	CFH	FN	TS	(N/mm)
JIC C1					
Preoperation	3.63	2.3	4.85	2.36	3068.48
Post-CTT	2.32 (-36.19%)	1.93 (-16.19%)	3.75 (-22.76%)	2.04 (-13.41%)	3356.89 (+ 9.40%)
Post-LBT	2.49 (-31.45%)	1.95 (-14.91%)	4.43 (-8.65%)	2.30 (-2.51%)	3227.45 (+ 5.18%)
JIC C2					
Preoperation	3.39	2.35	5.16	2.32	3205.67
Post-CTT	2.59 (-23.63%)	1.80 (-23.48%)	4.04 (-21.78%)	2.02 (-12.86%)	3454.55 (+ 7.76%)
Post-LBT	2.49 (-26.76%)	1.99 (-15.24%)	4.11 (-20.43%)	2.13 (-8.14%)	3278.12 (+ 2.26%)

WB: Weight-bearing area; CFH: Central femoral head; FH: Femoral neck; TS: Trochanteric and subtrochanteric region; The value in parentheses is the relative preoperative percentage.

The simulation of patient-specific models revealed that both the average von Mises stresses and stiffness decreased after LBT, which was consistent with the result of the healthy subject-derived models (Table 4). Compared with patient-1 (JIC Type C1), patient-2 (JIC Type C2) demonstrated greater changes in the above-mentioned parameters. As shown in Fig. 4b, the reduction of stresses in weight-bearing area was more obvious for patient-2. The postoperative X-ray radiography demonstrated that the femoral heads remained in shape (Fig. 3), and neither patient complained of hip pain in the 1-year follow-up.

Table 4
The average Von Mises stress and stiffness of patient-specific models

	Stress (Mpa)				Stiffness
	WB	CFH	FN	TS	(N/mm)
Patient-1					
preoperation	1.87	1.65	9.73	5.96	596.01
post-LBT	1.79 (-4.28%)	1.51 (-8.48%)	9.37 (-3.70%)	5.68 (-4.70%)	600.7 (+ 0.79%)
Patient-2					
preoperation	2.17	2.09	11.91	7.67	433.43
post-LBT	2.04 (-6.00%)	1.57 (-24.9%)	9.6 (-19.40%)	6.16 (-19.69%)	555.8 (+ 28.23%)

WB: Weight-bearing area; CFH: Central femoral head; FH: Femoral neck; TS: Trochanteric and subtrochanteric region; The value in parentheses is the relative preoperative percentage.

4. Discussion

Researchers on hip joint preservation surgeries of NONFH have tried to use finite element analysis to investigate the biomechanical performance of core decompression[24], rod implantation[27,28] and CTT[19]. However, there has been no such investigations of LBT. Although LBT has obtained relatively higher success rate in the treatment of NONFH[10], there are still concerns about its risk of fractures and comparisons among different techniques without evident warrant[14,8]. In this study, we performed finite element analysis of LBT in comparison with CTT, in order to provide biomechanical references for the current debates. Both LBT and CTT were calculated in their biomechanical aspect corresponding with the JIC classification.

In terms of validation of finite elemental models in this study, we compared our results with references and the physical character of the hip. Moreover, one patient in Type C1 and one patient in Type C2 were employed to validate the biomechanical properties of LBT. The shape and location of stress transfer path in this study is relevant to previous studies, which showed that stress transfer path was consistent with the distribution of bone density[19,29,30]. In addition, the average stress of weight-bearing area after fibula implantation, ranging from 2.32 to 2.59 Mpa, were in accordance with a recent study[28]. Therefore, the simulation results could reflect the physical status of the hip and could be used to analyze the effects of LBT and CTT.

The necrosis of femoral head varies from cases to cases, thus appropriate classification is prerequisite for the modelling. The JIC classification is a direct evaluation method to reflect the relative position

between necrotic lesions and the weight-bearing area[31–33], and has been proved to be an appropriated classification to predict stress distribution of the hip joint in vivo[19,30,34,35]. In the JIC classification, Type C1 and C2 are recommended to undergo joint-preserving therapies, so both types were employed in this study. Kuroda et al[16] reported that JIC classification could assist with the selection of therapeutic options before the collapse of the femoral head, particularly for patients with JIC Type C2 NONFH[35]. As Type C2 accounts for 53% of all NONFH[36] and is related to higher collapse rate recently[35], more emphasis should be placed on the treatment of this type.

In all postoperative finite element models, the average von Mises stresses were alleviated in the studied regions for both LBT and CTT. It is reasonable that the former necrotic areas were replaced by fibular grafts. Additionally, the stiffness increased in all models (Table 3), which indicated that both techniques could effectively improve structural stability of proximal femur and prevent the collapse of femoral head. These results were supported by the simulation of patient-specific models (Table 4 & Fig. 3). The stiffness of CTT was 4.01%-5.38% higher than that of LBT, which might be related to the different drilling ways and the length of grafted fibula. Note that, CTT needed a longer grafted fibula (Table 1).

The average stress of the weight-bearing area, indicating its collapse risk, is of the most importance in this study. Interestingly, different JIC groups showed opposite results (Table 3). In JIC C1 group, the average stress in the weight-bearing area of the femoral head after CTT was relatively lower, whereas LBT was relatively lower in JIC C2 group. The opposite result may be caused by the combination of several factors. Firstly, the tail of grafted fibula was partially supported by the lateral cortex of femur in LBT, while there was no such support by cortex in CTT. Secondly, in JIC C2 group, the angle formed between grafted fibula and stress transfer path was smaller than that in JIC C1 group, and the force transmitted to fibula was more, making the mechanical effect of LBT better than CTT in JIC C2 group. Moreover, cases of Type C2 patients account for the highest proportion (53%) in all types of NONFH, meaning that more patients received appropriate treatment in LBT. Maybe this is the reason why there were relative higher clinical success rates of LBT than CTT (94.6%-96% *vs* 60%-90%).

An assignable concern of surgeons regarding FVFG procedures is the structural defect at the proximal femur, which may cause the fracture of femoral neck and subtrochanteric regions potentially[12,37]. Aldridge et al[15] considered that LBT raised the stress by opening a window in the femoral neck. However, our results showed that the average stresses of femoral neck, trochanteric and subtrochanteric regions for LBT was lower than that preoperatively. Also, no yielding units appeared in these regions, meaning that the risk of fracture in these regions was reduced in LBT. Gao et al.[10] reported 578 hips with LBT procedure did not occur proximal femoral fractures postoperatively. However, as an comparative technique in this study, CTT was reported of 0.7%-1% fracture rate in previous studies[11,15,37], and those fractures all occurred in the intertrochanteric and subtrochanteric region after a fall[37]. Since the integrity of lateral femoral cortex is crucial to the structural strength against intertrochanteric and subtrochanteric fracture[38,39], the impact of CTT on this integrity needs further study. From our clinical experience, adequate postoperative rehabilitation and fall prevention may reduce the prevalence of fracture.

The limitation of this study should be clarified. Firstly, only one healthy hip joint model was used for simulation and two patient-specific models for validation. However, all comparisons were based on the healthy hip joint model, so the deviation caused by differences of models was eliminated. Secondly, our study used a simplified model, regardless of some reality details. For instance, we did not consider internal fixation for both LBT and CTT, instead, we considered that they had got bony union. However, our study focused on the structural changes of proximal femur as same as previous studies[19,40], the simplification would not affect the results. Last but not least, multiple factors affecting graft survival were not taken into consideration, such as the accuracy of surgery, revascularization realization, unbalance of creeping substitution, etc[41–43]. Further studies on the clinical comparison between LBT and CTT should combine these factors with biomechanical characteristics.

5. Conclusion

LBT and CTT have different biomechanical performance on different JIC type of NONFH. In terms of preventing the collapse of femoral head, LBT may be more effective for JIC C2 and could be chosen as an alternative, while CTT is still a better option for JIC Type C1. Biomechanical properties of NONFH can be improved by both techniques with patients' proximal femur stress reduced and structural stiffness enhanced.

List Of Abbreviations

Free Vascularized Fibula Graft (FVFG)

Nontraumatic Osteonecrosis of Femoral Head (NONFH)

Light Bulb Technique (LBT)

Core Track Technique (CTT)

Finite Element Analysis (FEA)

Japanese Investigation Committee (JIC)

Declarations

Ethics approval and consent to participate

CT image acquisitions were approved by Ethics Committee of Shanghai Sixth People's Hospital (Approval No. 2016-143) and written consents were obtained from participants.

Consent for publication

Participants enrolled into the study agreed the use of data for research.

Availability of data and materials

All of the data is available in contact with the correspondent author.

Competing interests

The authors declare that they have no competing interests.

Funding

This study was sponsored by the Interdisciplinary Program of Shanghai Jiao Tong University (YG2017QN14).

Authors' contribution

JX and SZ are responsible for finite element analysis, ML and DJ for data analysis, JX and SZ for manuscript writing, HH and JS for design of the study, surveillance of method and data quality, and manuscript writing. All authors have read and approved the manuscript for submission.

Acknowledgements

The authors appreciate Ling Xu for her helpful suggestions in language editing.

Author's information

Jian Xu, Email: nulidoudouxujian@hotmail.com

Shi Zhan, Email: zhanshi4890966@yeah.net

Ming Ling, Email: 19111280008@fudan.edu.cn

Dajun Jiang, Email: shiyingjiangdajun1@163.com

Hai Hu, Phone: +86 21 24058161, Email: xmhuhai@hotmail.com

Jiagen Sheng, Phone:+86 189 3017 4886 , Email: shengjiagen@126.com

Changqing Zhang, Phone: +86 21 24058161, Email: zhangcq@sjtu.edu.cn

References

1. Mont MA, Zywiel MG, Marker DR, McGrath MS, Delanois RE. The natural history of untreated asymptomatic osteonecrosis of the femoral head: a systematic literature review. *J Bone Joint Surg Am* 2010; **92**(12): 2165-70.
2. Eward WC, Rineer CA, Urbaniak JR, Richard MJ, Ruch DS. The vascularized fibular graft in precollapse osteonecrosis: is long-term hip preservation possible? *Clin Orthop Relat Res* 2012;

470(10): 2819-26.

3. Ohzono K, Saito M, Takaoka K, et al. Natural history of nontraumatic avascular necrosis of the femoral head. *J Bone Joint Surg Br* 1991; **73**(1): 68-72.
4. Cohen-Rosenblum A, Cui Q. Osteonecrosis of the Femoral Head. *Orthop Clin North Am* 2019; **50**(2): 139-49.
5. Zalavras CG, Lieberman JR. Osteonecrosis of the femoral head: evaluation and treatment. *J Am Acad Orthop Surg* 2014; **22**(7): 455-64.
6. Korompilias AV, Beris AE, Lykissas MG, Kostas-Agnantis IP, Soucacos PN. Femoral head osteonecrosis: why choose free vascularized fibula grafting. *Microsurgery* 2011; **31**(3): 223-8.
7. Cao L, Guo C, Chen J, Chen Z, Yan Z. Free Vascularized Fibular Grafting Improves Vascularity Compared With Core Decompression in Femoral Head Osteonecrosis: A Randomized Clinical Trial. *Clin Orthop Relat Res* 2017; **475**(9): 2230-40.
8. Wang J, Wang J, Zhang K, Wang Y, Bao X. Bayesian Network Meta-Analysis of the Effectiveness of Various Interventions for Nontraumatic Osteonecrosis of the Femoral Head. *Biomed Res Int* 2018; **2018**: 2790163.
9. Bassounas AE, Karantanas AH, Fotiadis DI, Malizos KN. Femoral head osteonecrosis: volumetric MRI assessment and outcome. *Eur J Radiol* 2007; **63**(1): 10-5.
10. Gao YS, Chen SB, Jin DX, Sheng JG, Cheng XG, Zhang CQ. Modified surgical techniques of free vascularized fibular grafting for treatment of the osteonecrosis of femoral head: results from a series of 407 cases. *Microsurgery* 2013; **33**(8): 646-51.
11. Aldridge JM, 3rd, Berend KR, Gunneson EE, Urbaniak JR. Free vascularized fibular grafting for the treatment of postcollapse osteonecrosis of the femoral head. Surgical technique. *J Bone Joint Surg Am* 2004; **86-A Suppl 1**: 87-101.
12. Ligh CA, Nelson JA, Fischer JP, Kovach SJ, Levin LS. The Effectiveness of Free Vascularized Fibular Flaps in Osteonecrosis of the Femoral Head and Neck: A Systematic Review. *J Reconstr Microsurg* 2017; **33**(3): 163-72.
13. Zhang C, Zeng B, Xu Z, et al. Treatment of femoral head necrosis with free vascularized fibula grafting: a preliminary report. *Microsurgery* 2005; **25**(4): 305-9.
14. Rosenwasser MP, Garino JP, Kiernan HA, Michelsen CB. Long term followup of thorough debridement and cancellous bone grafting of the femoral head for avascular necrosis. *Clin Orthop Relat Res* 1994; (306): 17-27.
15. Aldridge JM, 3rd, Urbaniak JR. Avascular necrosis of the femoral head: role of vascularized bone grafts. *Orthop Clin North Am* 2007; **38**(1): 13-22, v.
16. Sugano N, Atsumi T, Ohzono K, Kubo T, Hotokebuchi T, Takaoka K. The 2001 revised criteria for diagnosis, classification, and staging of idiopathic osteonecrosis of the femoral head. *Journal of orthopaedic science : official journal of the Japanese Orthopaedic Association* 2002; **7**(5): 601-5.

17. Nishii T, Sugano N, Ohzono K, Sakai T, Sato Y, Yoshikawa H. Significance of lesion size and location in the prediction of collapse of osteonecrosis of the femoral head: a new three-dimensional quantification using magnetic resonance imaging. *J Orthop Res* 2002; **20**(1): 130-6.
18. Urbaniak JR, Coogan PG, Gunneson EB, Nunley JA. Treatment of osteonecrosis of the femoral head with free vascularized fibular grafting. A long-term follow-up study of one hundred and three hips. *J Bone Joint Surg Am* 1995; **77**(5): 681-94.
19. Zhou G, Zhang Y, Zeng L, et al. Should thorough Debridement be used in Fibular Allograft with impaction bone grafting to treat Femoral Head Necrosis: a biomechanical evaluation. *BMC Musculoskelet Disord* 2015; **16**: 140.
20. Beris AE, Soucacos PN. Optimizing free fibular grafting in femoral head osteonecrosis: the Ioannina aiming device. *Clin Orthop Relat Res* 2001; (386): 64-70.
21. Reina-Romo E, Rodriguez-Valles J, Sanz-Herrera JA. In silico dynamic characterization of the femur: Physiological versus mechanical boundary conditions. *Med Eng Phys* 2018.
22. Lee MS, Tai CL, Senan V, Shih CH, Lo SW, Chen WP. The effect of necrotic lesion size and rotational degree on the stress reduction in transtrochanteric rotational osteotomy for femoral head osteonecrosis--a three-dimensional finite-element simulation. *Clin Biomech (Bristol, Avon)* 2006; **21**(9): 969-76.
23. Brown TD, Hild GL. Pre-collapse stress redistributions in femoral head osteonecrosis--a three-dimensional finite element analysis. *J Biomech Eng* 1983; **105**(2): 171-6.
24. Komistek RD, Stiehl JB, Dennis DA, Paxson RD, Soutas-Little RW. Mathematical model of the lower extremity joint reaction forces using Kane's method of dynamics. *J Biomech* 1998; **31**(2): 185-9.
25. Cilla M, Checa S, Preininger B, et al. Femoral head necrosis: A finite element analysis of common and novel surgical techniques. *Clin Biomech (Bristol, Avon)* 2017; **48**: 49-56.
26. Bayraktar HH, Morgan EF, Niebur GL, Morris GE, Wong EK, Keaveny TM. Comparison of the elastic and yield properties of human femoral trabecular and cortical bone tissue. *J Biomech* 2004; **37**(1): 27-35.
27. Shi J, Chen J, Wu J, et al. Evaluation of the 3D finite element method using a tantalum rod for osteonecrosis of the femoral head. *Med Sci Monit* 2014; **20**: 2556-64.
28. Huang L, Chen F, Wang S, et al. Three-dimensional finite element analysis of silk protein rod implantation after core decompression for osteonecrosis of the femoral head. *BMC Musculoskelet Disord* 2019; **20**(1): 544.
29. Boyle C, Kim IY. Three-dimensional micro-level computational study of Wolff's law via trabecular bone remodeling in the human proximal femur using design space topology optimization. *J Biomech* 2011; **44**(5): 935-42.
30. Wen PF, Guo WS, Zhang QD, et al. Significance of Lateral Pillar in Osteonecrosis of Femoral Head: A Finite Element Analysis. *Chin Med J (Engl)* 2017; **130**(21): 2569-74.
31. Takashima K, Sakai T, Hamada H, Takao M, Sugano N. Which Classification System Is Most Useful for Classifying Osteonecrosis of the Femoral Head? *Clin Orthop Relat Res* 2018; **476**(6): 1240-9.

32. Min BW, Song KS, Cho CH, Lee SM, Lee KJ. Untreated asymptomatic hips in patients with osteonecrosis of the femoral head. *Clin Orthop Relat Res* 2008; **466**(5): 1087-92.
33. Ito H, Matsuno T, Omizu N, Aoki Y, Minami A. Mid-term prognosis of non-traumatic osteonecrosis of the femoral head. *J Bone Joint Surg Br* 2003; **85**(6): 796-801.
34. Utsunomiya T, Motomura G, Ikemura S, et al. Effects of sclerotic changes on stress concentration in early-stage osteonecrosis: A patient-specific, 3D finite element analysis. *J Orthop Res* 2018; **36**(12): 3169-77.
35. Kuroda Y, Tanaka T, Miyagawa T, et al. Classification of osteonecrosis of the femoral head: Who should have surgery? *Bone Joint Res* 2019; **8**(10): 451-8.
36. Fukushima W, Fujioka M, Kubo T, Tamakoshi A, Nagai M, Hirota Y. Nationwide epidemiologic survey of idiopathic osteonecrosis of the femoral head. *Clin Orthop Relat Res* 2010; **468**(10): 2715-24.
37. Gaskill TR, Urbaniak JR, Aldridge JM, 3rd. Free vascularized fibular transfer for femoral head osteonecrosis: donor and graft site morbidity. *J Bone Joint Surg Am* 2009; **91**(8): 1861-7.
38. Palm H, Jacobsen S, Sonne-Holm S, Gebuhr P. Integrity of the lateral femoral wall in intertrochanteric hip fractures: an important predictor of a reoperation. *J Bone Joint Surg Am* 2007; **89**(3): 470-5.
39. Hsu CE, Shih CM, Wang CC, Huang KC. Lateral femoral wall thickness. A reliable predictor of post-operative lateral wall fracture in intertrochanteric fractures. *Bone Joint J* 2013; **95-b**(8): 1134-8.
40. Zhou GQ, Pang ZH, Chen QQ, et al. Reconstruction of the biomechanical transfer path of femoral head necrosis: a subject-specific finite element investigation. *Comput Biol Med* 2014; **52**: 96-101.
41. Meloni MC, Hoedemaeker WR, Fornasier V. Failed vascularized fibular graft in treatment of osteonecrosis of the femoral head. A histopathological analysis. *Joints* 2016; **4**(1): 24-30.
42. Gonzalez Della Valle A, Bates J, Di Carlo E, Salvati EA. Failure of free vascularized fibular graft for osteonecrosis of the femoral head: a histopathologic study of 6 cases. *J Arthroplasty* 2005; **20**(3): 331-6.
43. Fontecha CG, Roca I, Barber I, et al. Femoral head bone viability after free vascularized fibular grafting for osteonecrosis: SPECT/CT study. *Microsurgery* 2016; **36**(7): 573-7.

Figures

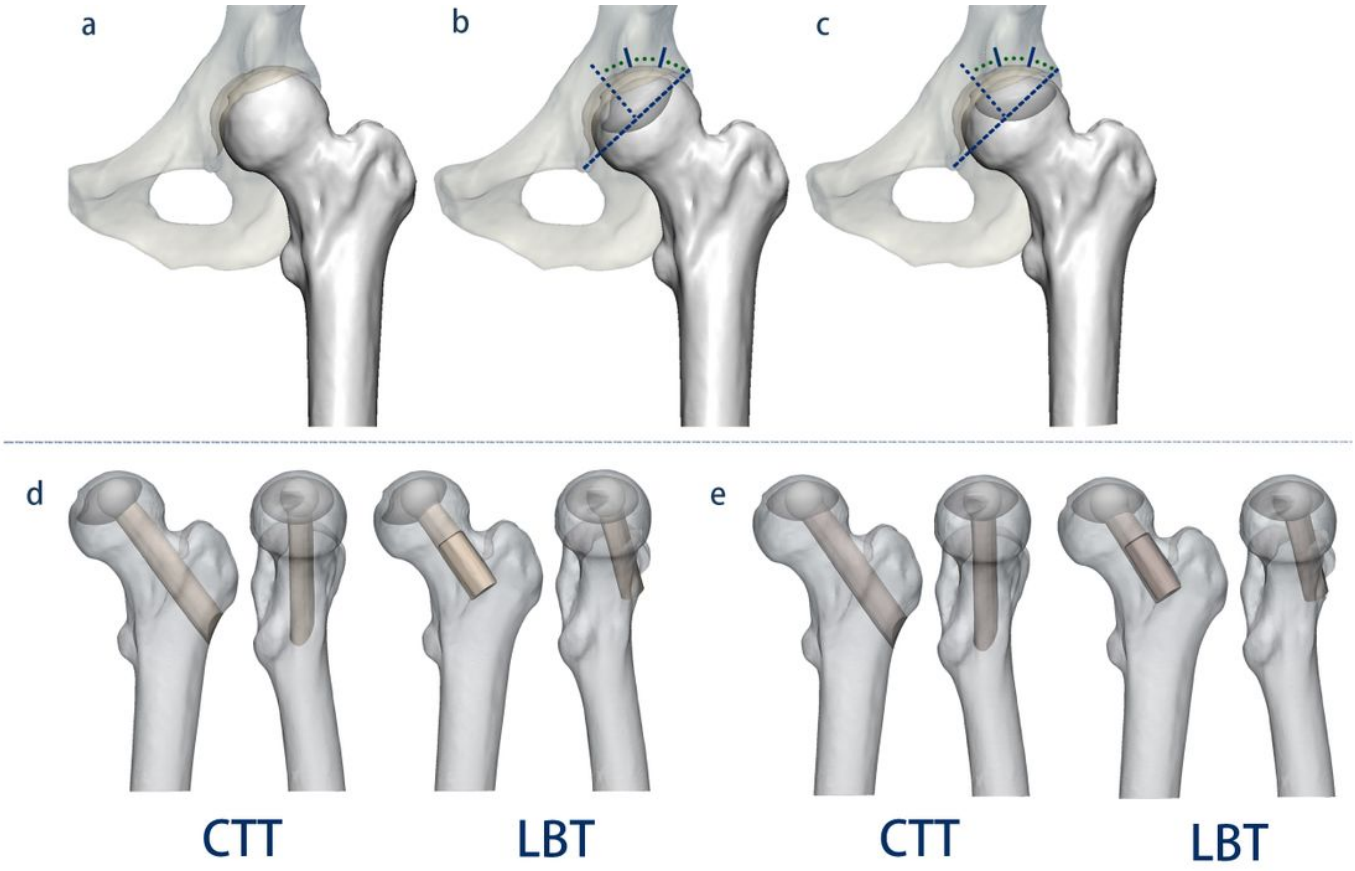

Figure 1

The healthy subject-derived models. (a) Reconstructed healthy hip model; (b) Japanese Investigation Committee (JIC) Classification Type C1: lesions occupy more than medial two thirds of the weight-bearing portion but do not extend laterally to the acetabular edge; (c) JIC Type C2: lesions occupy more than medial two-thirds of the weight-bearing portion and extend laterally to the acetabular edge. (d) The postoperative models on anteroposterior and medial-lateral views of the CTT and LBT in JIC C1 group. (e) The postoperative models on anteroposterior and medial-lateral views of the CTT and LBT in JIC C2 group.

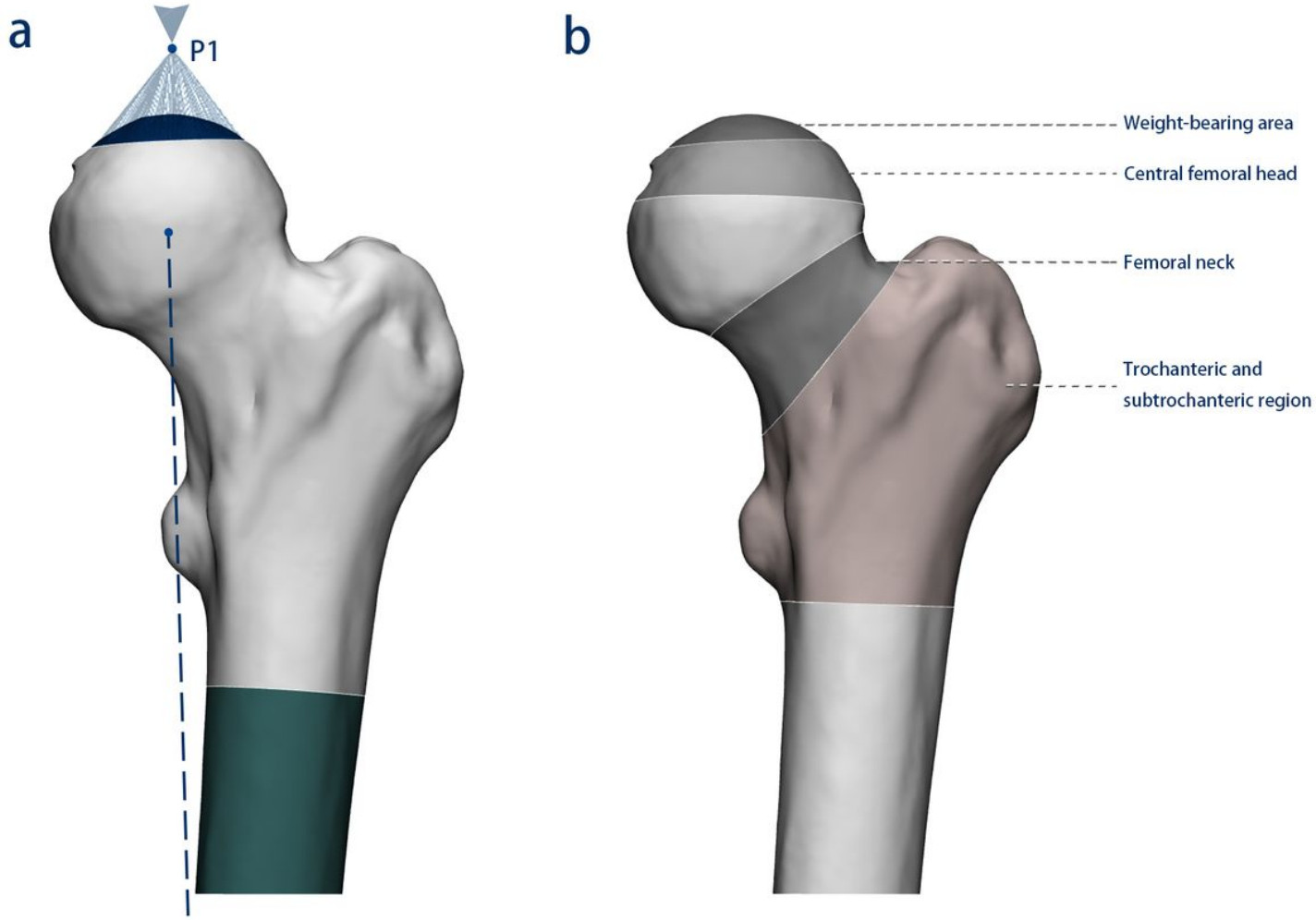

Figure 2

Boundary conditions and calculated regions in proximal femur. (a) 250% body weight was loaded on the reference point (P1) which was coupled with the entire weight-bearing area along the mechanical axis (dotted line) of the femur. The distal femur was fully restrained to movement. (b) Four regions were calculated include weight-bearing area, central femoral head, femoral neck and trochanteric and subtrochanteric regions.

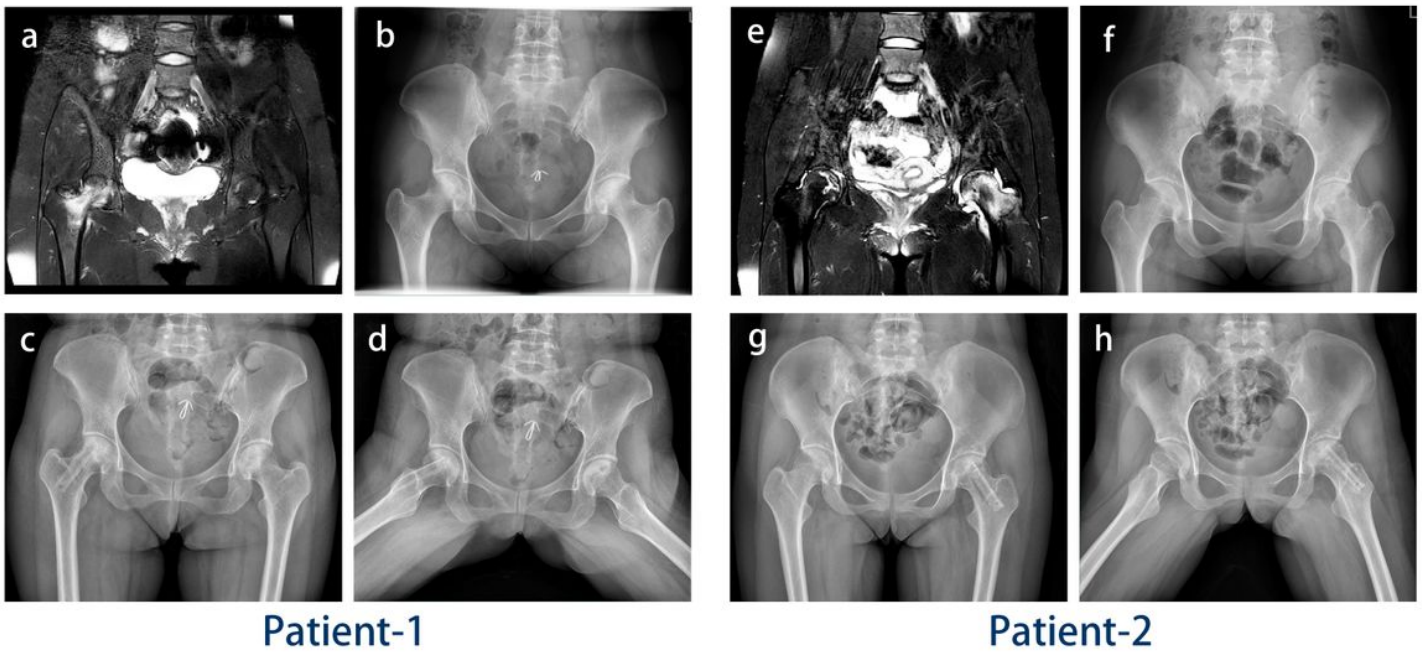

Figure 3

Two patients' pre-/post-operation images. (a-d) Patient-1, right hip was classified as NONFH JIC C1; (e-h) Patient-2, left hip was classified as NONFH JIC C2. Left-up panels (a, e) are preoperative T2-weighted MRI; right-up panels (b, f) are preoperative X-ray; low panels are postoperative X-ray, showing patient-1's right hip after LBT at 6 months follow-up (c, d), and patient-2's left hip after LBT at 4 weeks follow-up (g, h).

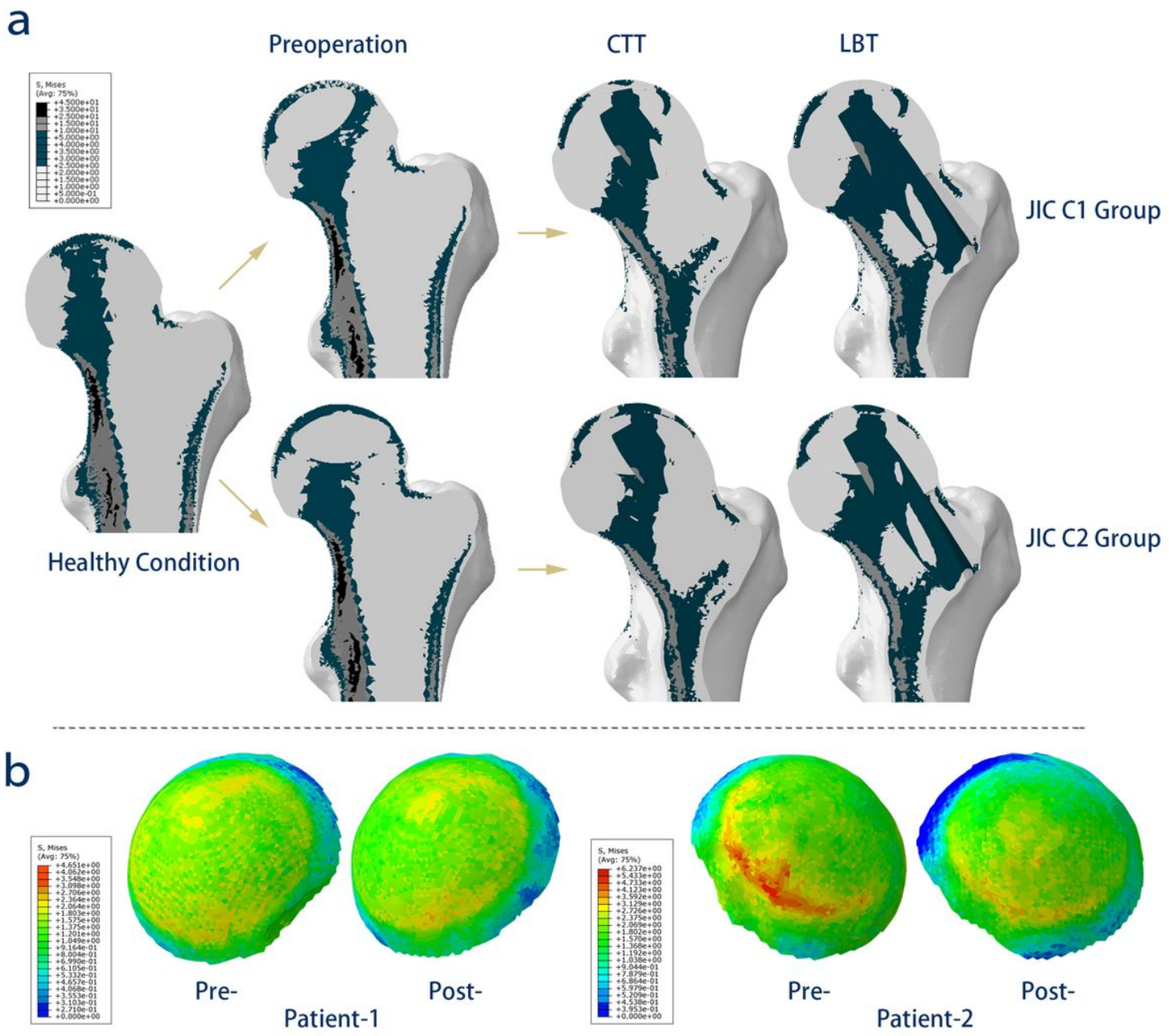

Figure 4

The stress distribution in finite element models. (a) The stress transfer path showed in healthy subject-derived models; preoperative models JIC C1 and JIC C2; postoperative models CTT and LBT were displayed in different necrotic groups. (b) The stress distribution of two patient-specific models in central femoral head region.

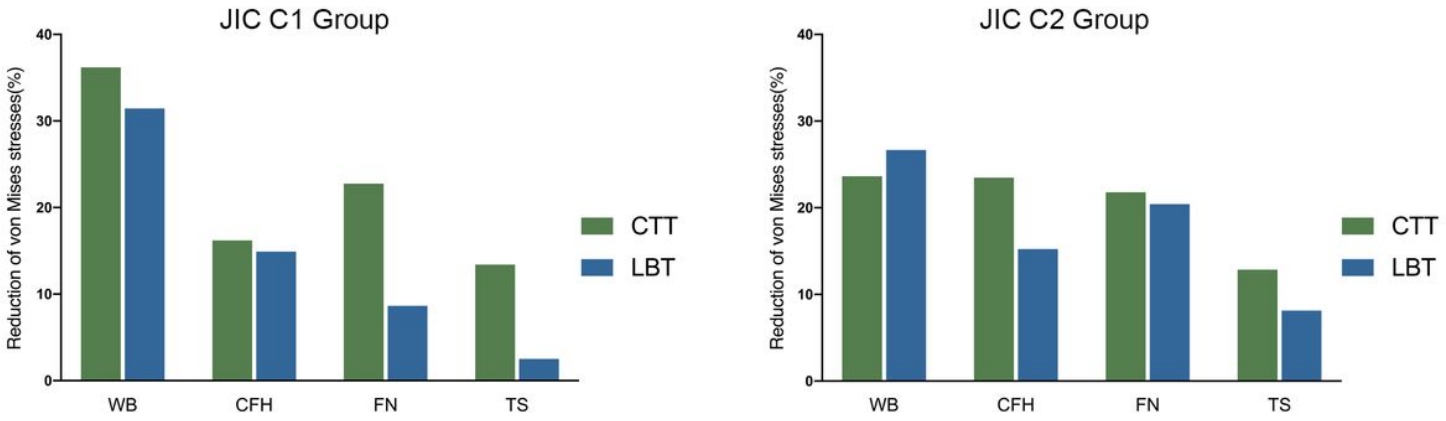

Figure 5

The reduction of average von Mises stresses following CTT/LBT in JIC C1 and C2 groups. CTT: Core Track Technique; LBT: Light Bulb Technique; WB: weight-bearing area; CFH: Central femoral head; FH: Femoral neck; TS: Trochanteric and subtrochanteric region.

Supplementary Files

This is a list of supplementary files associated with this preprint. Click to download.

- Formulas.pdf